Hydrodynamic Analysis of a Gliding Robotic Dolphin Based on Computational Fluid Dynamics

LI Kang, YU Junzhi, WU Zhengxing, and TAN Min

State Key Laboratory of Management and Control for Complex Systems,
Institute of Automation, Chinese Academy of Sciences, Beijing 100190, P. R. China
E-mail: likang2014@ia.ac.cn, junzhi.yu@ia.ac.cn, zhengxing.wu@ia.ac.cn, min.tan@ia.ac.cn

Abstract: This paper presents a concrete and practical hydrodynamic analysis for a hybrid gliding robotic dolphin. In order to obtain the accurate hydrodynamic performance of both dolphin-like swimming and gliding motion, a Computational Fluid Dynamics (CFD) method is employed. Specifically, based on the FlUENT dynamic mesh interface, a novel dynamic mesh and user-defined function (UDF) are developed to describe the dorsoventral oscillations of the dolphin. Besides, the corresponding turbulent model and SIMPLE algorithm suited to dolphin-like swimming are also meticulously selected for great accuracy and high quality. Finally, the FLUENT simulation results reveal the pressure distribution and velocity field distribution around the robotic dolphin. Moreover, some important hydrodynamic coefficients including lift coefficients and drag coefficients at different frequencies are also obtained. The simulation results illustrate an expected hydrodynamic performance of the gliding robotic dolphin.

Key Words: Gliding Robotic Dolphin, Computational Fluid Dynamics (CFD), Dynamic Mesh, Hydrodynamic Analysis

1 Introduction

Recent years have witnessed a growing interest in the study of biomimetic robots that imitate their body shapes and swimming abilities from underwater animals. Noticeably, with over half a billion years of evolution, aquatic swimmers are endowed with a variety of structural features for moving through water with astonishing speed, maneuverability and adaptability [1].

Dolphin, as a kind of aquatic animals, attracts much attention from numerous researchers. In particular, the efficient and flexible locomotion control methods and biology intelligences are concerned by them. Yu *et al.* [2] proposed a closed-loop pitch angle control strategy based on the intrinsic oscillatory property to realize excellent acrobatic maneuvers such as front-flip and back-flip (360° rotation in the vertical plane). Shen *et al.* [3] employed fuzzy PID control method to implement depth control of the robotic dolphin. Wang *et al.* [4] designed a central pattern generation (CPG)-based locomotion controller to implement multi-modal control for a robotic dolphin. Ren *et al.* [5] proposed an average propulsive speed implementation approach for robotic dolphins theoretically and experimentally. Wang *et al.* [6] developed a robotic dolphin with a voluntary movement function and artificial intelligence. Although these robotic dolphins can perform excellent dolphin-like swimming based on the proposed control strategies, some accurate hydrodynamic analyses always lacked. In order to obtain a more accurate performance estimation, it is required for robotic dolphin to execute hydrodynamic analysis in the process of motion especially the rhythmic motion using computational fluid dynamics (CFD).

The CFD simulation [7], as a significant fluid analysis tool, has been widely adopted to understand some complex physical phenomena like atmosphere flowing, turbulent motion and heat transmission with fast computer computation and detailed graphic exhibition. Lu *et al.* [8] employed CFD to simulate the non-uniform air flow distribution produced by an axial flow fan. Kumaresan *et al.* [9] analyzed the double walled cooking unit under different geometric and flow conditions by CFD. Ghadiri *et al.* [10] created a CFD model with ions transporting through membrane. Naturally, not only CFD simulations and analyses can be used on all above applications, but also have been carried out for robotic fishes. Mohammadshahi *et al.* [11] evaluated hydrodynamic forces of a fish-like swimming robot and optimized performance parameters in the process of design and fabrication based on the result by using a CFD model. Borazjani *et al.* [12] studied the hydrodynamics of a bluegill sunfish executing C-start maneuver using 3-D numerical simulations. Ma *et al.* [13] built a imitational tuna model and provided detailed hydrodynamic analysis. Zhou *et al.* [14] proposed a computational scheme to study bio-inspired fish swimming hydrodynamics through CFD model and designed a filtering algorithm to fuse near-body pressure of multiple points for the estimation on external flow field.

The objective of this paper is to present a novel hydrodynamic analysis for a hybrid gliding robotic dolphin. Feedback near-dolphin-body flow field information is of importance to enable underwater locomotion controllers with higher efficiency and adaptability within unknown environments. With inspiration from the natural dolphin sensing near-body flow field, we conduct this research. The movement pattern of the robotic dolphins is Thunniform included in the Body and/or Caudal Fin, which is different from a large number of propulsion modes of robotic fishes. Considering that numerous researches almost pay much attention to the robotic fishes and less concern of swimming of robotic dolphins, we focus on obtaining more accurate hydrodynamic properties of a gliding robotic dolphin. Based on our previous work [15], which only employed CFD methods to analyze the static gliding performance of the robotic dolphin, we realize dynamic dolphin-like swimming simulation through designing a innovative dynamic mesh and user-defined function (UD-

This work was partly supported by the National Natural Science Foundation of China (61375102, 61573226, 61333016, 61421004) and the Beijing Natural Science Foundation (3141002, 4164103), and partly supported by the Early Career Development Award of SKLMCCS.

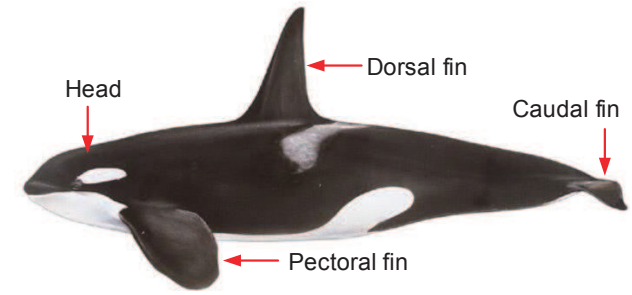

(a)

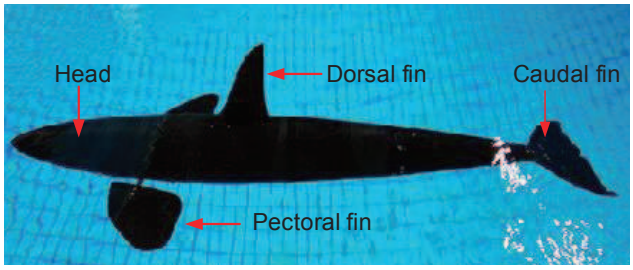

(b)

Fig. 1: The natural killer whale and prototype of the gliding robotic dolphin.

F). Besides, the corresponding turbulent model and SIMPLE algorithm well-suited to dolphin-like swimming are also meticulously selected for great accuracy and high quality. The FLUENT simulation results reveal the pressure distribution and velocity field distribution around the robotic dolphin. Simultaneously, some important hydrodynamic coefficients including lift coefficients and drag coefficients at different frequencies are also obtained. The simulation results illustrate an expected hydrodynamic performance of the gliding robotic dolphin.

The rest of this paper is organized as follows. The overall description of the gliding robotic dolphin is provided in Section 2. Section 3 gives the CFD simulation model including pre-processing meshing, applied turbulent model and boundary conditions, UDF and dynamic mesh parameters setting, as well as a SIMPLE algorithm. Section 4 presents the experiments and hydrodynamic analysis in detail. Finally, conclusion is drawn in Section 5.

2 Gliding Robotic Dolphin

The killer whale, as a member of cetaceans, can smartly utilize its strong and agile body to perform astonishing motions. Considering that the flexible and forced fins and dorsoventral oscillations in killer whale are efficient locomotor modes under water as well as gliding motion has long endurance and practical application, a gliding robotic dolphin has been developed. Figs. 1 (a) and (b) respectively show the natural killer whale and the prototype of the the gliding robotic dolphin which is composed of a head, two pectoral fins, a dorsal fin and a caudal fin.

The detailed mechanical designs are shown in Fig. 2. There are six principal cabinets interiorly including a head cabinet, a pectoral cabinet, a mission cabinet, a control cabinet, a waist cabinet and a caudal cabinet connected through wired electrical connection and wireless command connection with each other. The core propulsive units of exe-

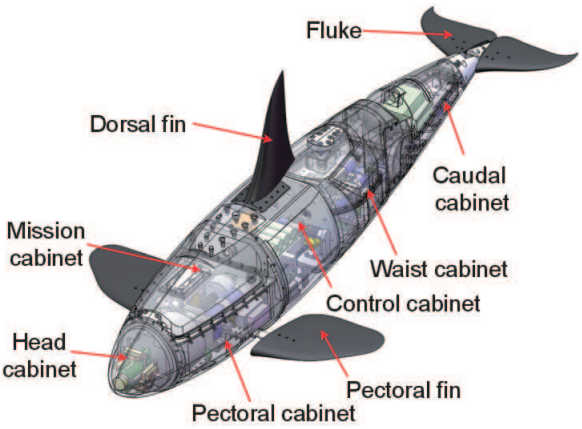

Fig. 2: Mechanical design of the gliding robotic dolphin [16].

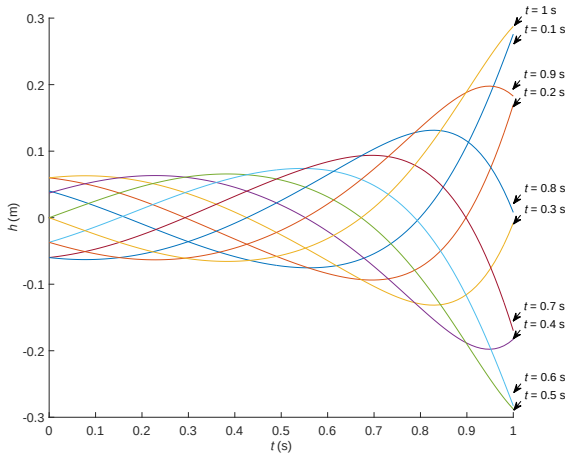

Fig. 3: Illustration of body wave during dolphin swimming.

cuting symmetrical sinusoidal dorsoventral oscillations are waist joint and caudal joint, where two powerful DC motors are utilized to drive the posterior dolphin body locomotion. Moreover, the waist cabinet also employed a yawing joint to implement turning maneuvers. On the other hand, the buoyancy-driven system is designed to realize the gliding motion, which consists of a DC motor for providing driving power, an emulsion bag in the protective shell for changing the buoyancy of the robotic dolphin and some connected mechanical parts for supporting achieving gliding motion. Generally, the robotic dolphin is 1.13 m long and weighs 18.20 kg. Adopting above-mentioned design with a well-streamlined body shape will help to improve the space utilization rate, lift-drag ratio and locomotion performance.

In order to improve endurance and practicability of the gliding robotic dolphin, a steady gliding motion is executed through changing buoyancy of the dolphin body. Simultaneously, to realize an efficient and effective dolphin-like swimming, an excellent and vivid dolphin body wave need to be applied to the robotic dolphin. As suggested by Romanenko [17], the periodic excursions of the body centerline in a dolphin swimming are approximated as

$$h(x_n,t) = h_T f(x_n)\sin(2\pi ft) \tag{1}$$

where h_T is the maximal vertical amplitude, $x_n = x/L$ is the

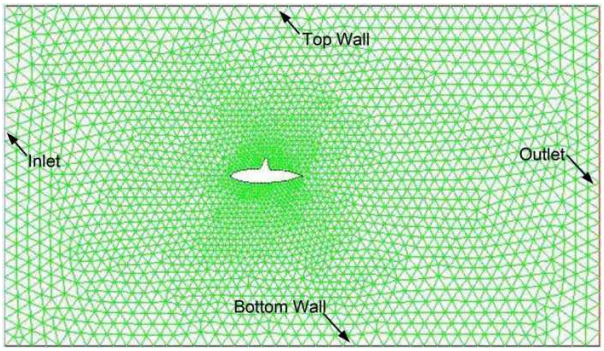

Fig. 4: 2D robotic dolphin mesh.

longitudinal coordinate measured from the beak, divided by the animals length L, $f(x_n)$ is the polynomial expression of x_n, taking a form of $0.21-0.66x_n+1.1x_n^2+0.35x_n^8$, f is the tail beat frequency, and t is time. Fig. 3 presents an oscillatory rhythm of the centerline of robotic dolphin over a period ($T = 1$ s).

3 CFD Simulation Model

3.1 Robotic dolphin mesh

Drawing mesh, as the first step of CFD analysis, is the key to a successful simulation. In consideration of the symmetrical, sinusoidal fluke oscillations in the vertical plane producing 90% of the total thrust, we designed a 2D robotic dolphin model which is enough to describe tail rhythmic motion. Fig. 4 presents the mesh model of robotic dolphin. In the pre-processing meshing work, an unstructured high qualified triangles mesh is formed by commercial software ANSYS 16.0 ICEM CFD to describe the flow domain. This meshing scheme give a lower number of meshes to reduce computation time.

3.2 Turbulent model and boundary conditions

In order to resolve viscous flow around a moving dolphin-like body, incompressible Navier-Stokes (NS) equations are the core for understanding fluid phenomena. Based on the CFD code description, the conservation form of the control equations can be written as

$$\frac{\partial \rho}{\partial t}+div(\rho \mathbf{u})=0 \tag{2}$$

$$\frac{\partial(\rho u)}{\partial t}+div(\rho u\mathbf{u})=div(\mu\, grad\, u)-\frac{\partial p}{\partial x}+S_u \tag{3}$$

$$\frac{\partial(\rho v)}{\partial t}+div(\rho v\mathbf{u})=div(\mu\, grad\, v)-\frac{\partial p}{\partial y}+S_v \tag{4}$$

$$\frac{\partial(\rho w)}{\partial t}+div(\rho w\mathbf{u})=div(\mu\, grad\, w)-\frac{\partial p}{\partial z}+S_w \tag{5}$$

where $div(\rho\mathbf{u})$ represents $\frac{\partial(\rho u)}{\partial x}+\frac{\partial(\rho v)}{\partial y}+\frac{\partial(\rho w)}{\partial z}$. t is time, ρ is density, p is pressure, μ is viscosity. u, v and w are velocity components in x, y and z axes. S_u, S_v and S_w are generalized source terms respectively.

In view of the turbulent flow generated by high Reynolds number, a k-ε two equations model [18] is built, which are defined as

$$\frac{\partial(\rho k)}{\partial t}+\frac{\partial(\rho k u_i)}{\partial x_i}=\frac{\partial}{\partial x_j}\left[\left(\mu+\frac{\mu_t}{\sigma_k}\right)\frac{\partial k}{\partial x_j}\right]+G_k-\rho\varepsilon \tag{6}$$

$$\begin{aligned}\frac{\partial(\rho\varepsilon)}{\partial t}+\frac{\partial(\rho\varepsilon u_i)}{\partial x_i}=&\frac{\partial}{\partial x_j}\left[\left(\mu+\frac{\mu_t}{\sigma_\varepsilon}\right)\frac{\partial \varepsilon}{\partial x_j}\right]\\&+\frac{C_{1\varepsilon}\varepsilon}{k}G_k-C_{2\varepsilon}\rho\frac{\varepsilon^2}{k}\end{aligned} \tag{7}$$

where ε is turbulent dissipation rate and k is turbulent kinetic energy, ρ is density, u_i is the temporal average velocity, μ is viscosity, $C_{1\varepsilon}$ and $C_{2\varepsilon}$ are empirical constant, σ_k and σ_ε are the turbulent Prandtl numbers for k and ε, respectively. G_k represents the generated term due to mean velocity gradients, can be calculated by

$$G_k=-\rho\overline{u'_i u'_j}\frac{\partial u_j}{\partial x_i} \tag{8}$$

The turbulent viscosity, μ_t can be computed by k and ε as:

$$\mu_t=\rho C_\mu\frac{k^2}{\varepsilon} \tag{9}$$

where C_μ is a constant, $C_{1\varepsilon}$, $C_{2\varepsilon}$, C_μ, σ_k and σ_ε are used by default value as $C_{1\varepsilon}=1.44$, $C_{2\varepsilon}=1.92$, $C_\mu=0.09$, $\sigma_k=1.0$ and $\sigma_\varepsilon=1.3$.

After establishing the discrete equations, the boundary conditions will be given. The whole computational domain of the dolphin body is surrounded by the following boundaries:

1) Inlet boundary: 2.5 folds body lengths from the nose to inlet boundary and set as velocity-inlet with $v=$ 0.3 m/s;
2) Outlet boundary: 2.5 folds body lengths from the fluke to outlet boundary and set as outflow;
3) Top and Bottom wall boundary: set as no-flip moving walls;
4) Surface boundary: set as interior.

3.3 UDF and dynamic mesh parameters setting

To simulate the robotic dolphin motion, we complete a novel dynamic mesh computation by using ANSYS 16.0 FLUENT solver. Dynamic mesh computation needs to solve two problems, the one is mesh regeneracy, the other is defining the motion or deforming of boundary.

For the first problem, we combine spring smoothing and remeshing method to deal with mesh severe variation due to robotic dolphin swimming. Parameters for setting dynamic mesh are shown in Table 1.

For the last problem, user-defined function is used to define the oscillation period of the robotic dolphin. We choose the DEFINE macro DEFINE_GRID_MOTION to describe the rhythmic oscillation of dolphin body, which is implemented according to Eq. 1 where h_T = 0.3 m, f = 1 Hz, and L = 1.08 m.

3.4 SIMPLE algorithm

SIMPLE is the short for Semi-Implicit Method for Pressure-Linked Equations, proposed by Patankar and Spalding [19] to solve the numerical simulation of incompressible fluid field. The core of SIMPLE algorithm is the loop process of surmise and modify, which implements computation of pressure field based on the cross mesh. The process of SIMPLE algorithm is described as follows. Firstly, solving discrete N-S equations to obtain velocity field based on the known pressure field. Because the initial pressure

Table 1: Parameters for Dynamic Mesh

Mesh methods	**Parameter setting**	
	Items	***Setting***
Smoothing	Spring constant factor	1
	Laplace node relaxation	1
	Convergence tolerance	0.001
	Number of iterations	20
Remeshing	Minimum length scale (m)	0.006
	Maximum length scale (m)	0.31
	Maximum cell skewness	0.7
	Maximum face skewness	0.7
	Size remeshing interval	5
	Sizing function resolution	3
	Sizing function variation	8.147
	Sizing function rate	0.3

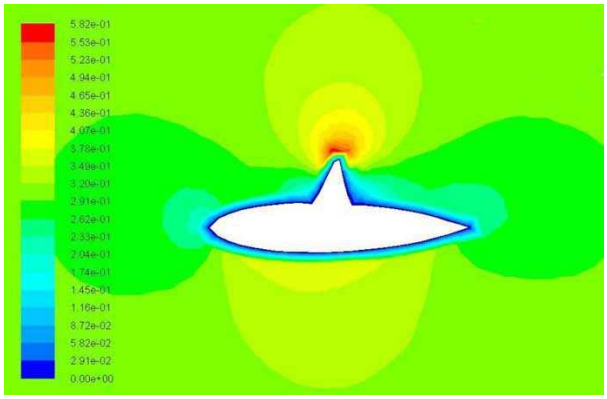

Fig. 5: Velocity contour of the gliding motion.

field is surmised and inaccuracy, the obtained velocity field usually fails to meet mass equation. For this reason, it is necessary to modify the initial pressure field, which needs modified pressure field corresponding velocity field to satisfy mass equation. According to this principle, pressure and velocity field iterate computation and modify over and over until convergence. As SIMPLE algorithm is convenient and effective in fluid computations, we employ it to solve pressure and velocity field around the robotic dolphin.

4 Experiment and Hydrodynamic Analysis

In this section, we will present two motion circumstances for the gliding robotic dolphin.

4.1 Gliding motion

The first experiment focused on the steady gliding motion at speed of 0.3 m/s in the vertical plane. Figs. 5 and 6 present the velocity and pressure contours. Results of simulation show two sides of robotic dolphin body (up-down) have the relative low static pressure but the maximal velocity. Instead, there is a maximal pressure and minimal velocity in the neighbouring of head. It is worth noting that the dorsal pin towards the incoming flow possesses maximal pressure, as well as the tip of the dorsal fin has maximal velocity. Based on the experiment results, we will improve the mechanical design including strengthening hardness of rigid of robotic dolphin head and dorsal fin.

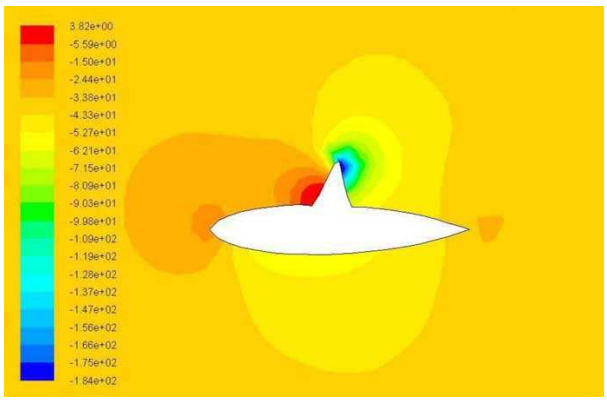

Fig. 6: Pressure contour of the gliding motion.

4.2 Dorsoventral oscillations

The second experiment focused on the swimming motion according to dolphin body wave. In the simulations, the robotic dolphin oscillates its tail at T = 1 s (swimming period). The velocity and dynamic pressure contours in different time of a period are shown in Figs. 7 and 8. We choose four moments to analyse the state of dolphin swimming respectively.

At the beginning, we focus on the velocity distribution. At $t = 0.05$ s, the dolphin tail achieves upwards maximal amplitude, the surrounding of dorsal fin presents considerable fluid velocity. The robotic dolphin body is going to swing from up to down. At $t = 0.4$ s, the right and up side of dolphin tail has a orange region, which means there is high velocity region. Meanwhile, an anti-clockwise vortex is formed. At $t = 0.65$ s, the dolphin tail achieves downwards maximal amplitude, the flush color of right and up side of the dolphin tail gets darker. The robotic dolphin body will swing from down to up. At $t = 0.95$ s, a period is approaching end, the dolphin tail generates a clockwise vortex and upward acceleration.

Then, the dynamic pressure distribution will be observed. At $t = 0.05$ s, a red region in the dorsal fin of robotic dolphin represents a big positive pressure, the dolphin tail achieves upwards maximal amplitude. Because of the start of oscillation, the left and down side of dolphin tail do not present positive pressure. However, there will be a red region on the left and down side of the dolphin tail in a rhythm movement. At $t = 0.4$ s, the right and up of dolphin tail appears positive pressure distribution, which illustrates a thrust of dolphin body along the directions of left-front is generated. At $t = 0.65$ s, on the right and up side of dolphin tail, the positive pressure seems to be increased. The dolphin tail achieves downwards maximal amplitude. At $t = 0.95$ s, on the left and down side of dolphin tail, positive pressure is increasing, which implies the trend of swinging is from the down to up. A thrust of dolphin body along the directions of right-front is generated by the movement of caudal fin.

All above hydrodynamic analyses describe the motion rhythm of robotic dolphin over a period, which almost consists of the all kinds of dolphin swimming states. The force acting on the tail of robotic dolphin can be divided into two types, the thrust at forward direction and the drag at up-down direction. As the force analysis plays a considerably important role of the hydrodynamic analysis, we plot diagrams of

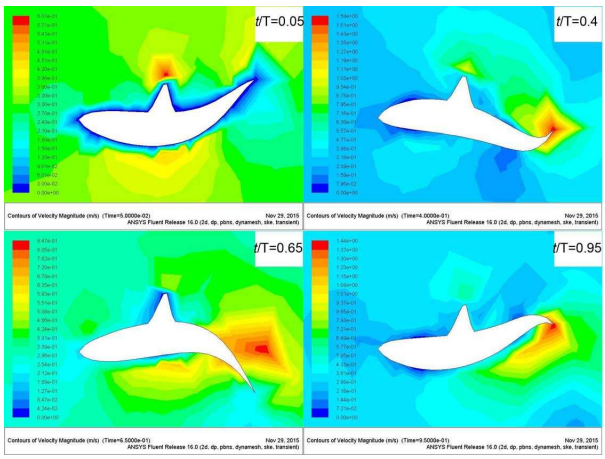

Fig. 7: Velocity contour of the swimming motion.

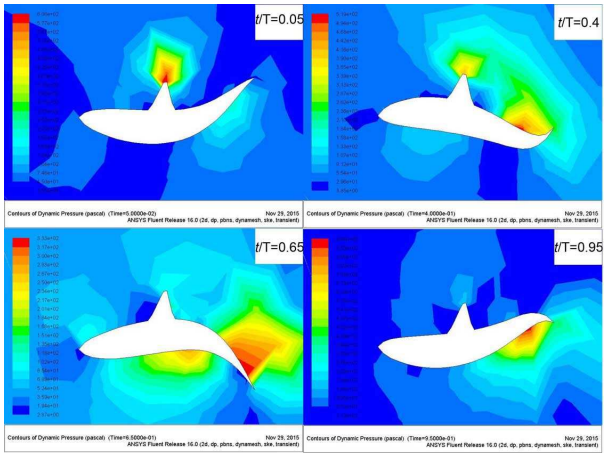

Fig. 8: Pressure contour of the swimming motion.

the drag and lift force coefficient varied with time, which are shown in Fig. 9. Around $t = 0.05$ s and $t = 0.65$ s, absolute values of c_l and c_d run up to considerable numbers, which means angle of attack reaches ideal position and pose of float and dive. Around $t = 0.4$ s and $t = 0.95$ s, we can observe c_d value has a small fluctuation near 0, the state is suitable to accelerate thrust. As regards the tiny fluctuation, it may be effected by turbulence.

4.3 Force analysis

In order to observe the force acting on dolphin body in different tail oscillating movement frequencies, a comparative experiment is executed. Figs. 9–11 show the hydrodynamic coefficients with different moments and frequencies respectively. From the diagrams, we found that the waves trend of hydrodynamic coefficients are almost identical, but absolute values of c_l and c_d turn to bigger with the frequency increasing. This represents that the higher the robotic dolphin tail swinging frequency, the quicker the swimming speed of the robotic dolphin, which is consistent with the understanding of swimming propulsion.

4.4 Discussion

Obtaining accurate hydrodynamic parameters of the gliding robotic dolphin is intractable without CFD numerical simulations. In our previous work, the static analyses of

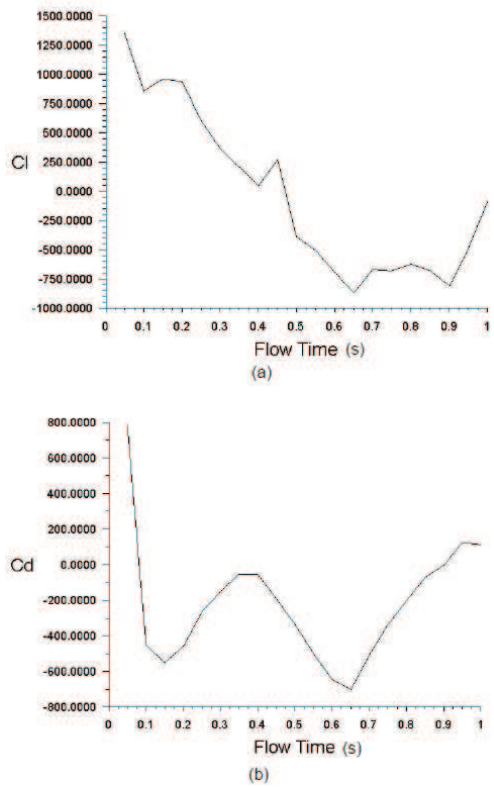

Fig. 9: Computed temporal variation of force coefficient for the tail motion ($f = 1$ Hz). (a) lift coefficient, (b) drag coefficient.

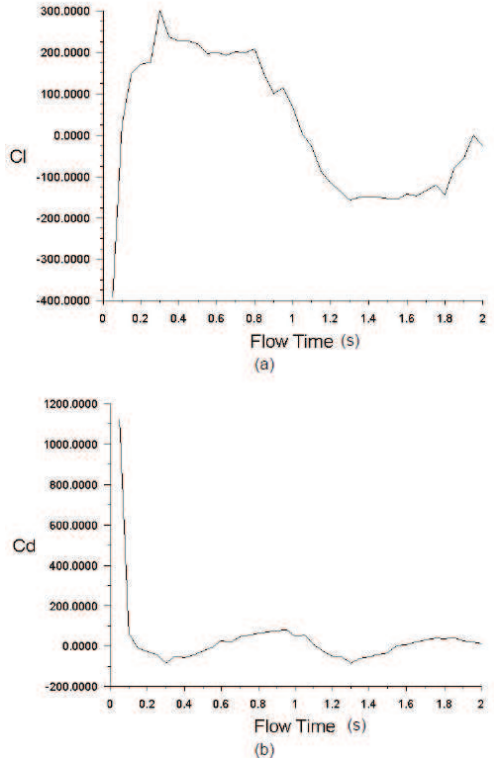

Fig. 10: Computed temporal variation of force coefficient for the tail motion ($f = 0.5$ Hz). (a) lift coefficient, (b) drag coefficient.

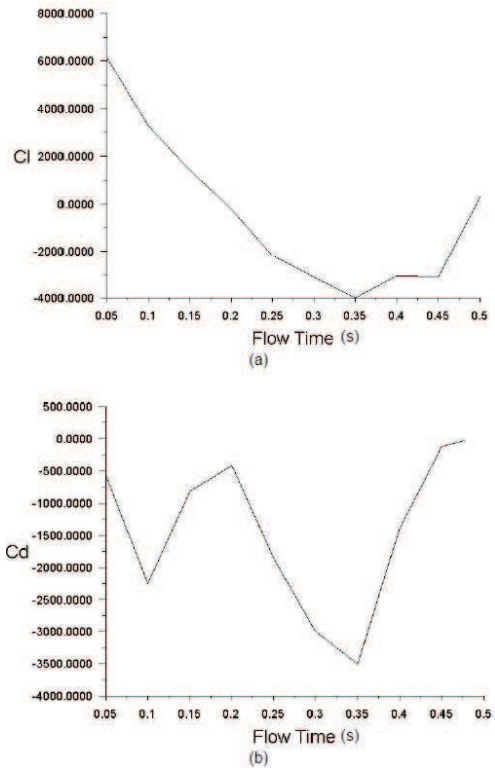

Fig. 11: Computed temporal variation of force coefficient for the tail motion ($f = 2$ Hz). (a) lift coefficient, (b) drag coefficient.

the gliding robotic dolphin are executed. The hydrodynamic force coefficients are decided by various factors such as the angle of attack, sideslip angle, Reynolds number of the flow and so on. Compared with our previous work, the dynamic mesh computation of the robotic dolphin effectively solves the near-dolphin-body pressure and velocity distributions, as well as obtains the expected dolphin-like swimming performance. In fact, with the amelioration of control algorithm and prediction of hydrodynamic coefficients from the dynamic CFD simulation in various motion types, the robotic dolphin will performs excellently.

5 Conclusion

In this paper, we have implemented a novel computational fluid dynamics simulation of a gliding robotic dolphin. Based on the previous static hydrodynamic analysis, we build the dynamic mesh interface and design UDF functions especially for dolphin-like swimming. Both turbulent model and SIMPLE algorithm have also been demonstrated in detail. It is easy to realize an excellent hydrodynamic performance including steady gliding motion and dorsoventral oscillation. Meanwhile, vital and accurate hydrodynamic parameters including pressure field, velocity field and drag-lift coefficients are obtained. Extensive experiments have illustrated reasonableness of the hydrodynamic simulation and analysis of the gliding robotic dolphin.

The future work will concentrate on the three-dimensional CFD simulation of the robotic dolphin and replication of more complex motions like turning or leaping out of the water in certain unknown underwater environments.

References

[1] F. E. Fish and J. J. Rohr, Review of dolphin hydrodynamics and swimming performance, *SPAWARS System Center Technical Report 1801*, 1999.

[2] J. Yu, Z. Su, M. Wang, M. Tan, and J. Zhang, Control of yaw and pitch maneuvers of a multilink dolphin robot, *IEEE Transactions on Robotics*, 28(2): 318–329, 2012.

[3] F. Shen, Z. Cao, C. Zhou, et al, Depth control for robotic dolphin based on fuzzy PID control, *International Journal of Offshore and Polar Engineering*, 23(03), 2013.

[4] M. Wang, J. Yu, M. Tan, H. Wang, and C. Li, CPG–based multi–modal swimming control for robotic dolphin, *Acta Automation Sinica*, 40(9): 1933–1941, 2014.

[5] G. Ren, Y. Dai, Z. Cao, et al, Research on the implementation of average speed for a bionic robotic dolphin, *Robotics and Autonomous Systems*, 74: 184–194, 2015.

[6] Y. L. Wang, C. H. Tai, and H. R. Huang, Design and development of an autonomous underwater vehicle–robot dolphin, *Journal of Marine Engineering & Technology*, 14(1): 44–55, 2015.

[7] J. Tu, G. H. Yeoh, C. Liu, *Computational Fluid Dynamics: A Practical Approach*, Butterworth–Heinemann, 2012.

[8] H. Lu, X. Xue, X. Tang, et al, CFD analysis of the non-uniform velocity distribution generated by a large axial flow fan, *ASME 2015 Pressure Vessels and Piping Conference. American Society of Mechanical Engineers*, 2015.

[9] G. Kumaresan, G. Raju, S. Iniyan, et al, CFD analysis of flow and geometric parameter for a double walled solar cooking unit, *Applied Mathematical Modelling*, 39(1): 137–146, 2015.

[10] M. Ghadiri, M. Asadollahzadeh, A. Hemmati, CFD simulation for separation of ion from wastewater in a membrane contactor, *Journal of Water Process Engineering*, 6: 144–150, 2015.

[11] D. Mohammadshahi, A. Yousefi-Koma, S. Bahmanya, et al, Design, fabrication and hydrodynamic analysis of a biomimetic robot fish, *Proceedings of WSEAS International Conference on Mathematics and Computers in Science and Engineering*, 2008.

[12] I. Borazjani, F. Sotiropoulos, E. D. Tytell, and G. V. Lauder, Hydrodynamics of the bluegill sunfish C-start escape response: three-dimensional simulations and comparison with experimental data, *The Journal of Experimental Biology*, 215(4): 671–684, 2012.

[13] Y. Ma, H. Zhao, Numerical Simulation Analysis of Biomimetic Robotic Fish Based on CFD, *Journal of Baicheng Normal University*, 5: 005, 2014.

[14] H. Zhou, T. Hu, K. H. Low, et al, Bio-inspired flow sensing and prediction for fish-like undulating locomotion: A CFD-aided approach, *Journal of Bionic Engineering*, 12(3): 406–417, 2015.

[15] Z. Wu, J. Yu, Z. Su, et al, Design and CFD analysis for a biomimetic dolphin-like underwater glider, *Proceedings of 2015 International Conference on CLAWAR*, 2015: 736–743.

[16] Z. Wu, J. Yu, J. Yuan, M. Tan, et al, Mechatronic design and implementation of a novel gliding robotic dolphin, *Proceedings of 2015 IEEE International Conference on Robotics and Biomimetics(ROBIO)*, 2015: 267–271.

[17] E. V. Romanenko, *Fish and Dolphin Swimming*, Pensoft, 2002.

[18] B. E. Launder, D. B. Spalding, Lectures in mathematical models of turbulence, 1972.

[19] S. V. Patankar, D. B. Spalding, A calculation procedure for heat, mass and momentum transfer in three-dimensional parabolic flows, *International Journal of Heat and Mass Transfer*, 15(10): 1787–1806, 1972.